



Increases in dendritic spine density in BLA without metabolic changes in a rodent model of PTSD

Laura Tartari Neves^{1,2} · Paula Fernanda Ribas Neves^{1,2} · Lisiê Valéria Paz^{1,2} · Mariana Zancan³ · Bruna Bueno Milanesi¹ · Gabriele Zenato Lazzari¹ · Rafaela Barboza da Silva¹ · Marina Mena Barreto Peres de Oliveira¹ · Gianina Teribele Venturin⁴ · Samuel Greggio⁴ · Jaderson Costa da Costa⁴ · Alberto A. Rasia-Filho³ · Régis Gemerasca Mestriner^{1,2} · Léder Leal Xavier^{1,2}

Received: 21 January 2019 / Accepted: 13 August 2019 / Published online: 22 August 2019
© Springer-Verlag GmbH Germany, part of Springer Nature 2019

Abstract

Imaging studies have shown abnormal amygdala function in patients with posttraumatic stress disorder (PTSD). In addition, alterations in synaptic plasticity have been associated with psychiatric disorders and previous reports have indicated alterations in the amygdala morphology, especially in basolateral (BLA) neurons, are associated with stress-related disorders. Since, some individuals exposed to a traumatic event develop PTSD, the goals of this study were to evaluate the early effects of PTSD on amygdala glucose metabolism and analyze the possible BLA dendritic spine plasticity in animals with different levels of behavioral response. We employed the inescapable footshock protocol as an experimental model of PTSD and the animals were classified according to the duration of their freezing behavior into distinct groups: “extreme behavioral response” (EBR) and “minimal behavioral response”. We evaluated the amygdala glucose metabolism at baseline (before the stress protocol) and immediately after the situational reminder using the microPET and the radiopharmaceutical ¹⁸F-FDG. The BLA dendritic spines were analyzed according to their number, density, shape and morphometric parameters. Our results show the EBR animals exhibited longer freezing behavior and increased proximal dendritic spines density in the BLA neurons. Neither the amygdaloid glucose metabolism, the types of dendritic spines nor their morphometric parameters showed statistically significant differences. The extreme behavior response induced by this PTSD protocol produces an early increase in BLA spine density, which is unassociated with either additional changes in the shape of spines or metabolic changes in the whole amygdala of Wistar rats.

Keywords PTSD · Amygdaloid complex · Dendritic spines · ¹⁸F-FDG · MicroPET

Introduction

According to the Diagnostic and Statistical Manual of Mental Disorders (DSM-5), Posttraumatic stress disorder (PTSD) is a psychiatric condition classified in the “Trauma and Stressor-Related Disorders” category (American Psychiatric Association 2013). PTSD is a debilitating disorder that develops after exposure to a traumatic event which involves threatened death, serious injury or sexual violence. The psychophysiological symptoms of PTSD are associated with the traumatic event and include avoidance, negative thoughts and mood and alterations in arousal and reactivity. These symptoms persist more than a month and cause significant impairment in patients’ lives (American Psychiatric Association 2013; Shalev et al. 2017). In addition, DSM-5 recognizes a dissociative subtype of PTSD, where patients present

✉ Léder Leal Xavier
llxavier@pucrs.br

¹ Laboratório de Biologia Celular e Tecidual, Escola de Ciências, Pontifícia Universidade Católica do Rio Grande do Sul (PUCRS), Av. Ipiranga 6681, Prédio 12C, Sala 104, Porto Alegre, Rio Grande do Sul CEP 90619-900, Brazil
² Programa de Pós-Graduação em Biologia Celular e Molecular, Pontifícia Universidade Católica do Rio Grande do Sul (PUCRS), Porto Alegre, Rio Grande do Sul, Brazil
³ Departamento de Ciências Básicas/Fisiologia, Universidade Federal de Ciências da Saúde de Porto Alegre, Porto Alegre, Rio Grande do Sul, Brazil
⁴ Instituto do Cérebro do Rio Grande do Sul (InsCer), Pontifícia Universidade Católica do Rio Grande do Sul (PUCRS), Porto Alegre, Rio Grande do Sul, Brazil

depersonalization and derealization in addition to the other classical symptoms.

Epidemiological studies show a high prevalence of traumatic exposure in individuals over a lifetime (Benjet et al. 2016; Kessler et al. 1995), and some individuals, when confronted with severe traumatic events, develop PTSD (Kessler et al. 1995; Yehuda et al. 2015).

As in humans, animals also demonstrate individual differences in their response following stress. Animals submitted to the same protocol may show higher or lower levels of response to stress (Bush et al. 2007; Cohen et al. 2003, 2004). Thus, some studies have classified animals into distinct groups according to their behavior: animals that exhibit higher levels of stress and anxiety were classified as “EBR—extreme behavioral response” and those with lower responses were classified as “MBR—minimal behavioral response” (Cohen et al. 2014; Saur et al. 2017).

The amygdaloid complex is closely involved in PTSD and plays an important role in the neuronal circuits involved in fear, anxiety and emotional reactions (Rasia-Filho et al. 2000; Tovote et al. 2015; Fenster et al. 2018). Indeed, some imaging studies reported abnormal amygdala function in patients with PTSD, showing increased metabolism in the amygdala in these patients (Shin et al. 2005; Rauch et al. 2000).

The microPET combined with the radiopharmaceutical ^{18}F -FDG (microPET-FDG), a metabolic analogue glucose marker, is a non-invasive imaging technique widely used in both patients and rodent models of PTSD studies, which allows the quantification of encephalic glucose metabolism (Saur et al. 2017; Yehuda et al. 2009; Virdee et al. 2012; Lancelot and Zimmer 2010; Zhu et al. 2016). Evaluating the glucose metabolism at different moments of PTSD, such as during the traumatic event and when this event is remembered is a difficult task, thus, microPET-FDG can be useful to evaluate the activity of the amygdala at these different time points.

Recent studies involving acute, subacute or chronic stress models have reported alterations in the synaptic function and neuroarchitecture that are associated to stress-related disorders (Patel et al. 2018; Musazzi et al. 2018; Zhang et al. 2018; Shu and Xu 2017). In addition, alterations in the morphology of the basolateral amygdala (BLA) neurons were found to be related to fear and anxiety in animal models (Vyas et al. 2002, 2004; Mitra and Sapolsky 2008; Mitra et al. 2009).

Dendritic spines are highly plastic and can change their density and morphology in a relatively short time, according to different stimuli (Gipson and Olive 2017). These changes in spine density can affect synaptic function since the number of spines is thought to be related to neuronal connectivity and excitability (Cooke and Woolley 2005; Yuste 2013; Dalpian et al. 2015). In addition, the shape and size of the

spines might also influence the neuronal connections, since thin spines are smaller, transient and considered “learning spines” whereas mushroom spines have more stability, greater postsynaptic density and are associated with stronger synapses (Leuner and Shors 2013; Bourne and Harris 2007). Ramified spines can have functional microdomains in the same spine, while atypical spines represent transient forms or additional levels of structural complexity for synaptic processing (Chen and Sabatini 2012; Dall’Oglio et al. 2015; Zancan et al. 2018).

Animal models are currently accepted as useful tools to better understand the biological features of diseases. Here, we chose the electric footshock (FS) protocol to mimic some PTSD features and analyze individual differences in stress response. The FS protocol is widely used to generate long-lasting effects commonly seen in PTSD patients, such as intrusive memories (fear generalization), avoidance, anhedonia and hyperarousal (Borghans 2015; Flandreau and Toth 2017).

To achieve our goal, the animals were classified according to the duration of their individual freezing response into two distinct groups: “extreme behavioral response” (EBR) and “minimal behavioral response” (MBR). Thus, we evaluated the early effects of an animal model of PTSD on amygdala glucose metabolism using microPET with ^{18}F -FDG and analyzed the number, density, shape and morphometric parameters of the BLA dendritic spines.

Materials and methods

Animals

Twenty-nine male, 3-month old Wistar rats were obtained from the Centro de Modelos Biológicos Experimentais (CEMBE) of the Pontifícia Universidade Católica do Rio Grande do Sul (PUCRS) and kept in standard laboratory conditions in the University’s facilities, with food and water ad libitum and a 12 h light/dark cycle. Animals were divided into three groups, according to a behavioral cut-off criterion previously described in Saur et al. (2017). The mean freezing time of the rodents that received the footshock was measured (mean = 42 s) and the animals that froze for over 42 s were classified as EBR ($n = 12$), while animals that froze for less than 42 s were classified as MBR ($n = 10$). In addition, rodents that did not receive the footshock were classified as control ($n = 7$). All experiments involving animals were approved by the University’s ethical committee (CEUA 8481/PUCRS) and were in accordance with the Guide for the Care and Use of Laboratory Animals adopted by the National Institute of Health (USA). All efforts were made to minimize animal suffering and the number of animals needed.

Experimental model of PTSD (single inescapable footshock)

The experimental model used in this study was based on previous research by Saur et al. (2017). Briefly, a single inescapable footshock was used to induce an experimental model of PTSD. For the experiment, animals were individually placed in an apparatus which consists of a 50 × 25 × 25 cm box with a bronze grid floor. The animals were permitted to explore the apparatus for 2 min prior to receiving a 20-s, 1 mA 60 Hz footshock. Animals in the control group were also placed in the apparatus but did not receive the footshock.

Body weight gain after stress protocol

To estimate the body weight gain after the stress induction, the body weight was recorded twice: once before the stress protocol and again, 7 days after the stress protocol.

Situational reminder (SR) and group division

One week after the aversive stimulus protocol (Fig. 1), animals were exposed to the situational reminder (SR) to evaluate the duration of freezing behavior, which is a measure of conditioned fear. To achieve this goal, animals were again placed in the same apparatus, but no shock was delivered. Two experienced researchers observed the animals in the apparatus for 2 min and measured the amount of time each animal exhibited freezing behavior. The animals were divided into three groups, according to the same cut-off behavioral criterion described by Saur et al. (2017). They were classified in extreme behavioral response (EBR), minimal behavioral response (MBR) or control, according to the treatment and freezing period.

MicroPET-FDG scan

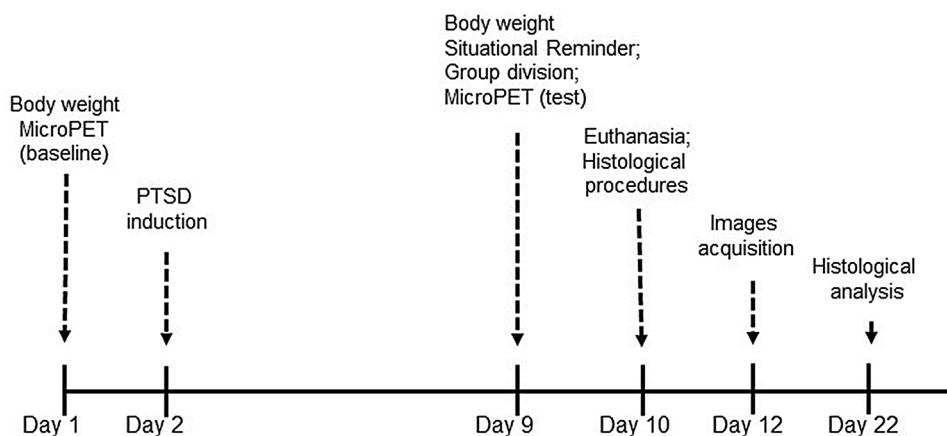
All the animals from the three experimental groups were submitted to microPET-FDG scanning at two different

time points: On the first day of the experiments, to evaluate their basal metabolic activity in the amygdala, and on day 9, immediately after the SR (Fig. 1). The microPET scanning procedure has been previously described in detail in other studies by our group (Saur et al. 2017; Baptista et al. 2015). Initially, each animal received an injection of ^{18}F -FDG (1 mCi, i.p.) with no anesthesia and, immediately after, they were submitted to the SR to evaluate the freezing behavior. Thereby, the encephalic uptake of the tracer occurred during the performance of the behavioral test. After the SR, the animals were returned to the home cage for an additional 30 min to finalize the tracer uptake. After the uptake period (40 min in total), the animals were scanned over a period of 10 min, during which they were kept under inhalatory anesthesia (3–4% isoflurane and medical oxygen, and 2–3% maintenance dose) and the body temperature was maintained at 36 °C. All data were reconstructed using the maximum likelihood estimation method (MLEM-3D) algorithm with 20 iterations. Each reconstructed microPET image was spatially normalized into an ^{18}F -FDG template using brain normalization in PMOD Fuse It Tool (PFUSEIT) 3.8 version (PMOD Technologies, Zurich, Switzerland). An MRI rat brain volume of interest (VOI) template was used to overlay the normalized images, previously co-registered to the microPET image database. We evaluated the ^{18}F -FDG uptake in the amygdala. The results were normalized by the whole brain and expressed as relative standardized uptake value (SUVr).

Euthanasia and histological procedures

On day 10 (Fig. 1), animals were deeply anesthetized with sodium thiopental (100 mg/kg) and lidocaine (4 mg/kg, i.p.). After which, transcardiac perfusion was performed using a peristaltic pump after an injection of 1 ml of heparin in the left ventricle of the animals. 250 ml of 1.5% formaldehyde diluted in 0.1 M phosphate buffer (PB, pH 7.4) were perfused in each animal and the brains were gently removed

Fig. 1 Timeline depicting the experimental procedures



from the skull and kept for 1 h in the same fixative solution. Coronal brain sections (200 μm) of the basolateral amygdala (BLA) (Bregma – 2.04 mm to Bregma – 2.76, Paxinos and Watson 2014, Fig. 2a) were obtained using a vibrating microtome (VT 1000S, Leica, Germany). Fine-powdered fluorescent carbocyanine dye Dil (Molecular Probes, USA) was applied to the slices using the tip of a fine needle. Then the slices were covered with PBS and remained for 20 h at room temperature (RT) to diffuse the Dil. 4% formaldehyde solution was used to postfix the slices for 30 min prior to being washed with PB. The slides were mounted with “Fluoromount G” (“antifading medium solution”, refractive index = 1.4, Electron Microscopy, Sciences, USA) and the images were acquired within the following week (Zancan et al. 2018; Brusco et al. 2010; Rasia-Filho et al. 2010).

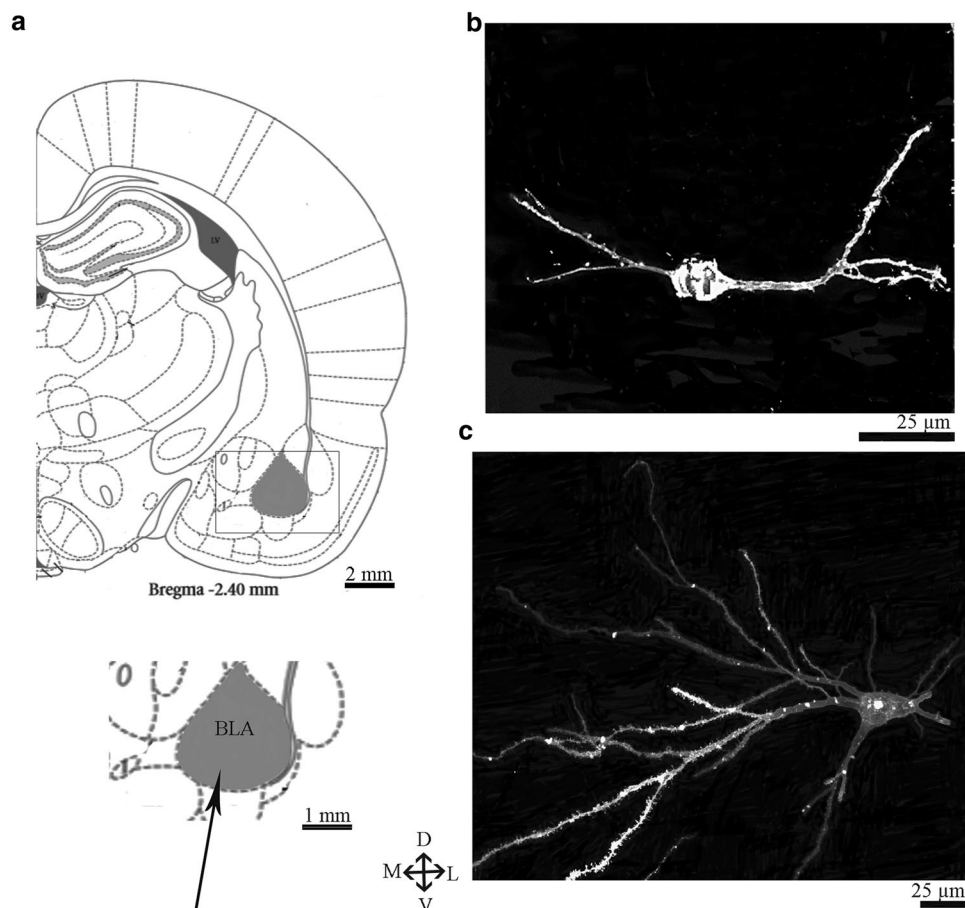
Image acquisition

3D images of the BLA neurons and their proximal dendritic spines were obtained from 6 rats per group using a confocal microscope (Leica TCS SP8, Germany) with a plan apochromatic 63 \times /1.4 water-immersion objective lens. Spectral detectors were adjusted to capture 555 nm wavelength laser emissions. The z-stack acquisition was performed at 0.1 μm

using a resolution of 1024 \times 1024 pixels, providing a voxel size of approximately 55 \times 55 \times 300 nm (Zancan et al. 2018; Brusco et al. 2010). Neurons were selected for further study using the following inclusion criteria: (1) being located within the boundaries of the BLA and near the middle third of the section; (2) having primary dendrites extending at least 40 μm from the cell body (since our analysis was performed in the first 40 μm of the primary branch); (3) presenting high quality fluorescent dendrites and spines with well-defined borders; and, (4) being relatively isolated from other cells to avoid “tangled” dendrites. Both BLA bitufted (Fig. 2b) and stellate (Fig. 2c) non-pyramidal neurons were randomly sampled. 5–17 neurons per rat from each experimental group were obtained. One primary dendrite per neuron was randomly selected and imaged for the dendritic spine counting, classification and measurements in the first 40 μm of the selected primary branch.

Note that some bitufted or stellate neurons could not be classified in either group due to overlapping images. Despite which these neurons were included in our analysis because they belong to the group of non-pyramidal neurons, the main target of our study. The proportion of types of neurons in our study was: bitufted (control group = 16.12%/MBR = 19.35%/EBR = 17.18%); stellate (control group = 53.22%/

Fig. 2 **a** Schematic diagram of a brain section showing the BLA (at –2.40 mm posterior to the bregma) marked in grey. Adapted from Paxinos and Watson Rat Brain Atlas (2014). **b** Digitalized image showing a BLA bitufted neuron. **c** Digitalized image showing a BLA stellate neuron



MBR = 45.16%/EBR = 62.5%) and neurons with overlapping images (control group = 30.64%/MBR = 35.48%/EBR = 20.31%).

Histological analysis

The images were analyzed using the Image Pro Plus 6.0 software. Data were collected on the density, shape and structural morphometric parameters of each dendritic spine (Zancan et al. 2017, 2018; de Castilhos et al. 2008). Each acquired sequence of z stacks was summed and aligned to compose 3D images. The same sampling density for pixel size and z -step advance and the same image acquisition procedures were performed for all experimental groups (Zancan et al. 2018; Heck et al. 2012). To analyze the spine shape and density, the images were enhanced by 200 \times and each spine was classified and counted by an experienced researcher. Morphological criteria based on the spine length (SL), neck length (NL), neck diameter (ND), head diameter (HD) and the number of protrusions from a single stalk were used to classify the spines in (a) thin (when $SL > HD$ and $HD > ND$), (b) mushroom-like ($HD \gg ND$), (c) stubby/wide ($HD > SL$), (d) ramified (with a single stalk with two or more spine heads) or (e) atypical (when showing a transitional aspect between classes or an unusual shape not classified in the other classes (Dall'Oglio et al. 2015; Zancan et al. 2017, 2018; Brusco et al. 2010, 2014; Harris et al. 1992; Arellano et al. 2007; Stewart et al. 2014). The spine density was calculated as the total number of spines (including all spine types) divided by the length of the dendrite studied. The number of spines in each type was also determined. Morphometric data (measured in micrometers) about the SL, NL, ND and HD were also obtained after further enhancing the 3D reconstructed images by 400 \times (Zancan et al. 2018; Rasia-Filho et al. 2004).

Spine length was measured as the distance from the dendritic shaft to the top of the spine. The spine neck and head diameter corresponded to the maximum distance perpendicular to the long axis of each these parts of the spine (Zancan et al. 2018; Ryu et al. 2006).

The investigator was blind to the groups during these analyses.

Statistical analysis

The data regarding the microPET-FDG scans and the dendritic spines were first submitted to a two-way ANOVA test to compare the experimental groups, brain hemispheres and the interaction of these two factors. Since no difference was found for the effect of hemispherical laterality or the interaction between factors, results from the right and left amygdala were pooled together and compared between groups.

One-way ANOVA for repeated measures was used to assess freezing behavior duration and the microPET-FDG, both followed by Tukey's post hoc test. The percentage of the body weight gain was analyzed using the Kruskal–Wallis test followed by the Dunn's post hoc test. One-way ANOVA followed by Tukey's post hoc test was performed for the spine density, number of each spine type per group and their corresponding morphometric values. Pearson's correlation test was used to analyze the correlation between freezing behavior, total spine density and ^{18}F -FDG activity. Parametric data are presented as mean \pm SEM while non-parametric measurements are presented as median and interquartile range. The results were considered significant when $p \leq 0.05$. GraphPad Prism 5.0 software was used to perform the analyses.

Results

The statistical analysis revealed stress had a significant effect on the percentage of body weight gain ($KW_{(2,28)} = 7.269$; $p \leq 0.05$). The Dunn's post hoc test showed the animals from the EBR group increased the percentage of body weight gain when compared to the controls (difference in rank sum = -9.64 ; $p \leq 0.05$). There was no significant difference between the MBR and control groups (difference in rank sum = -1.893 ; $p \leq 0.05$), or between the EBR and MBR groups (difference in rank sum = -7.750 ; $p \leq 0.05$) as seen in Fig. 3.

The duration of freezing behavior measured during the SR are shown in Fig. 4a. Before the stress protocol (i.e. at baseline), animals of all three groups did not present freezing behavior at any time point ($p = 1.0$). The repeated measures ANOVA (groups comparison between baseline versus post-shock) revealed that the inescapable footshock changes the freezing behavior (time effect: $F_{(1,26)} = 154.2$; $p \leq 0.0001$; partial eta squared = 0.856/group effect: $F_{(2,27)} = 62.86$; $p \leq 0.0001$; partial eta squared = 0.829/time \times group

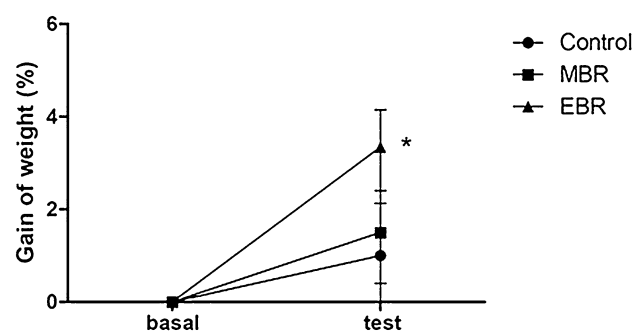


Fig. 3 Body weight gain (in percentage) after the stress protocol. Note a significant increase in this parameter when the EBR group is compared to the control group ($p < 0.05$)

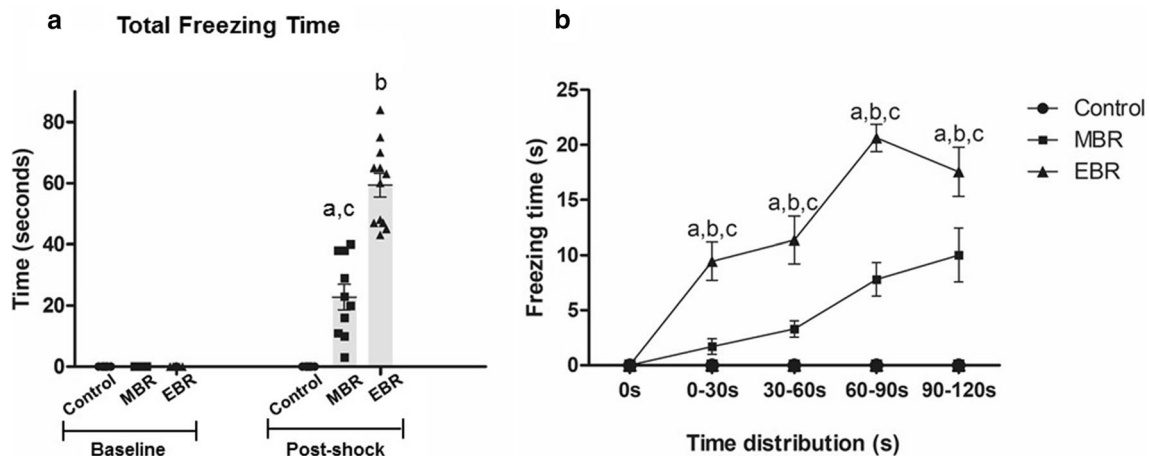


Fig. 4 a The duration of total freezing time measured before the stress protocol (i.e.) baseline and after the stress protocol. **a** At baseline, no animals from any of the three groups presented freezing behavior. After the stress, both the EBR and MBR groups showed longer duration of freezing time when compared to the control group. Additionally, the duration of freezing behavior was longer in the

EBR when compared with the MBR group. **a**=MBR versus control ($p \leq 0.001$); **b**=EBR versus control ($p \leq 0.0001$) and **c**=EBR versus MBR ($p \leq 0.0001$) and **b** distribution of freezing behavior during the entire 2 min of the test, plotted at intervals of 30 s. **a**=MBR versus control ($p \leq 0.002$); **b**=EBR versus control ($p \leq 0.0001$) and **c**=EBR versus MBR ($p \leq 0.0001$)

interaction effect: $F_{(2,26)} = 62.86$; $p \leq 0.0001$; partial eta squared = 0.829). The post hoc test showed the EBR group (Cohen_d = 6.28; $r = 0.95$; $p \leq 0.0001$) and the MBR group (Cohen_d = 2.44; $r = 0.77$; $p \leq 0.001$) differed from the controls, as denoted by a longer duration of the freezing time. Moreover, the animals from the EBR group remained frozen longer than those from the MBR group (Cohen_d = 2.766; $r = 0.81$; $p \leq 0.0001$).

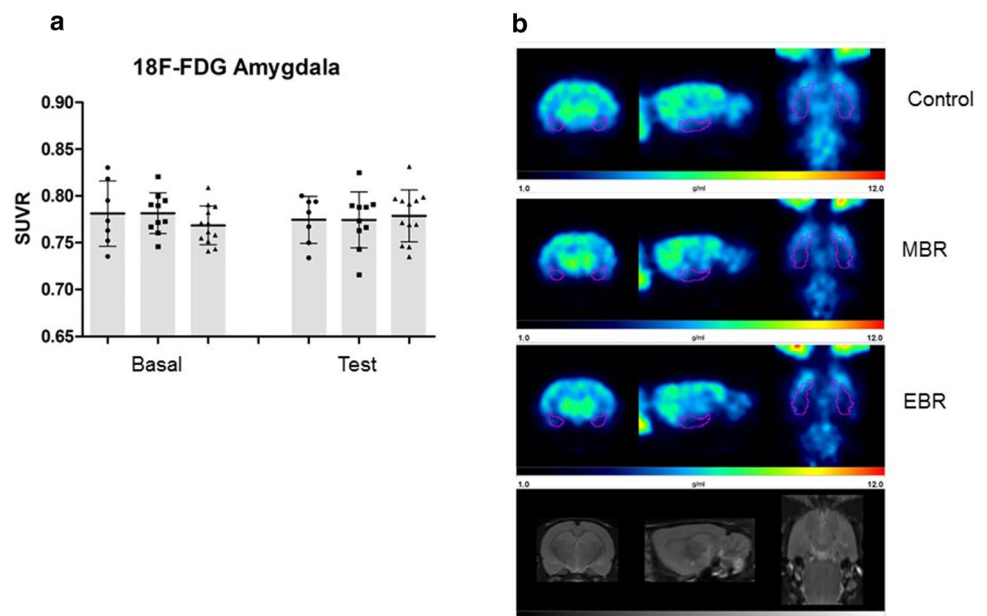
Additionally, Fig. 4b shows a more detailed examination of the freezing distribution during the entire 2 min, plotted at intervals of 30 s. After the stress protocol, the MBR and EBR groups showed an overall increase in freezing behavior over time (time effect: $F_{(4,27)} = 22.80$; $p \leq 0.000$; partial eta squared = 0.47/group effect: $F_{(2,27)} = 57.28$; $p \leq 0.0001$; partial eta squared = 0.82/time \times group interaction effect: $F_{(8,27)} = 8.01$; $p \leq 0.0001$; partial eta squared = 0.39). Moreover, the EBR group was different from the MBR and the controls in all the assessed intervals ($p \leq 0.0001$). The MBR was also different from the controls in the same assessed time-points ($p \leq 0.002$). Thus, we demonstrate that the PTSD inducing protocol is capable of generating fear behavior and does not affect all animals equally.

The glucose metabolism in the amygdala, analyzed by the mean ¹⁸F-FDG SUVr are shown in Fig. 5. The animals were submitted to the microPET scanning at two different time points. On day 1, before the experimental procedures, to evaluate the basal metabolic activity and 8 days after, to observe the effects of the PTSD protocol on the amygdala glucose metabolism during the SR. The one-way ANOVA for repeated measures showed no statistically significant differences in the ¹⁸F-FDG SUVr data between the groups

($F_{(2,26)} = 0.63$; $p = 0.54$) and time \times group interaction ($F_{(2,26)} = 0.47$; $p = 0.63$).

The number, size and shape of the dendritic spines in the BLA from all the experimental groups were studied (Figs. 6, 7). The statistical analysis revealed a significant increase in the spine density ($F_{(2,17)} = 3.84$; $p = 0.045$), showing that the animals in the EBR group had more proximal dendritic spines when compared with the animals from the control group (mean difference = -0.16; $q = 3.92$; $p < 0.05$; effect size_(d-Cohen) = 1.13), as shown in Fig. 8a. Dendritic spines classified as stubby/wide, thin and mushroom-like spines were the most common types found in the BLA neurons, although there was no statistically significant difference in the number of each type of spine between the groups (thin: $F_{(2,17)} = 2.125$; $p = 0.153$ /mushroom: $F_{(2,17)} = 3.385$; $p = 0.061$ /stubby/wide: $F_{(2,17)} = 1.503$; $p = 0.254$ /ramified: $F_{(2,17)} = 1.827$; $p = 0.195$ /atypical: $F_{(2,17)} = 0.690$; $p = 0.516$) (Fig. 8b). Also, total spine length (thin: $F_{(2,17)} = 0.095$; $p = 0.909$ /mushroom: $F_{(2,17)} = 0.242$; $p = 0.787$ /stubby/wide: $F_{(2,17)} = 0.504$; $p = 0.613$ /ramified: $F_{(2,17)} = 1.955$; $p = 0.176$ /atypical: $F_{(2,17)} = 0.440$; $p = 0.651$), neck length (thin: $F_{(2,17)} = 0.063$; $p = 0.939$ /mushroom: $F_{(2,17)} = 1.835$; $p = 0.193$ /ramified: $F_{(2,17)} = 1.486$; $p = 0.257$), head diameter (thin: $F_{(2,17)} = 1.189$; $p = 0.331$ /mushroom: $F_{(2,17)} = 0.694$; $p = 0.514$ /stubby/wide: $F_{(2,17)} = 0.123$; $p = 0.884$ /ramified: $F_{(2,17)} = 0.347$; $p = 0.712$), and neck diameter (thin: $F_{(2,17)} = 0.666$; $p = 0.528$ /mushroom: $F_{(2,17)} = 0.802$; $p = 0.466$ /ramified: $F_{(2,17)} = 0.443$; $p = 0.649$ /atypical: $F_{(2,17)} = 0.597$; $p = 0.562$) did not differ in any spine type among the groups (Fig. 9a–d).

Fig. 5 **a** ^{18}F -FDG uptake in the amygdaloid complex. The results are expressed as standard uptake value ratio (SUVr). **b** ^{18}F -FDG rat brain image in coronal (left), sagittal (mid), and transverse (right) views of all three groups and microMRI rat template in coronal (bottom-left), sagittal (bottom-mid), and transverse (bottom-right) views. The amygdala, outlined in purple, was defined using a rat ROI-template based on Paxinos coordinates



We found a positive correlation between the freezing time and the percentage of body weight gain ($r=0.4963$; $r^2=0.2463$; $p<0.01$) (Fig. 10a) and also between freezing time and spine density ($r=0.5336$; $r^2=0.2848$; $p<0.05$) (Fig. 10b). No correlation was found between freezing time and ^{18}F -FDG activity (Fig. 10c); spine density and the percentage of body weight gain (Fig. 10d) or spine density and ^{18}F -FDG activity (Fig. 10e).

Discussion

In our study, we show that, as observed in humans, animals can express individual differences in their behavioral responses when exposed to a situational trauma. The inescapable footshock protocol used to induce PTSD symptoms revealed that the animals were not equally affected, as shown by the different durations of freezing behavior.

Our results demonstrate that animals classified in the EBR and MBR groups showed longer duration of freezing behavior when compared to the control group. Moreover, animals from the EBR group remained more time in freezing when compared with animals from the MBR group. These findings support previous reports which showed that stressed animals submitted to the same protocol can either remain unaffected or exhibit different levels of fear behavior (Cohen et al. 2003, 2004, 2014; Saur et al. 2017; Mitra et al. 2005), even in inbred lines (Krishnan et al. 2007). In addition, a closer examination of the animals' fear behavior revealed an increase in the time spent freezing in the MBR and EBR groups, as presented in Fig. 4b. Ours results indicate that, at least in the initial two minutes of the SR test, the freezing response increases along with the test. One hypothesis to

explain this phenomenon could be an increase in activity in the brain regions responsible for the freezing behavior (Fanselow 1994; Mongeau et al. 2003; Wei et al. 2015; Silva et al. 2016).

The reasons for this resilience or susceptibility remain unknown, although some studies suggest that the susceptibility to develop stress-related disease is associated with genetic factors, early life stress, past experience, microbiome and the individual neurobiology (Mitra et al. 2005; Heim and Nemeroff 2001; Diehl et al. 2007; McEwen 2008; Adamec et al. 2012; Luczynski et al. 2016; Malan-Muller et al. 2018). Considering that all the animals studied here were from the same strain and reared under the same standard laboratory conditions prior to beginning the experiments, the present data indicate a likely innate variability in the response to aversive stimulation within Wistar rats.

The EBR group showed a significant increase in body weight gain when compared to the control group, which was positively correlated with the freezing time. In rodents, stress protocols can produce the full range of responses in relation to body weight, no difference (Saur et al. 2016), weight loss (Vallès et al. 2000; Jiang et al. 2011) or weight gain (Goto et al. 2014). One explanation for the weight gain found in our study might be related to a possible increase in serum corticosterone levels, leading to increased food and water intake and sodium reabsorption induced by the mineralocorticoid effects of corticosterone. Future studies using similar stress protocols evaluating serum corticosterone levels and food/water intake shed some light on this point. Interestingly, the increase in body weight gain observed in the EBR group is similar to findings reported in patients with PTSD. In fact, several studies have shown that PTSD can predispose to weight gain and obesity (Kubzansky et al.

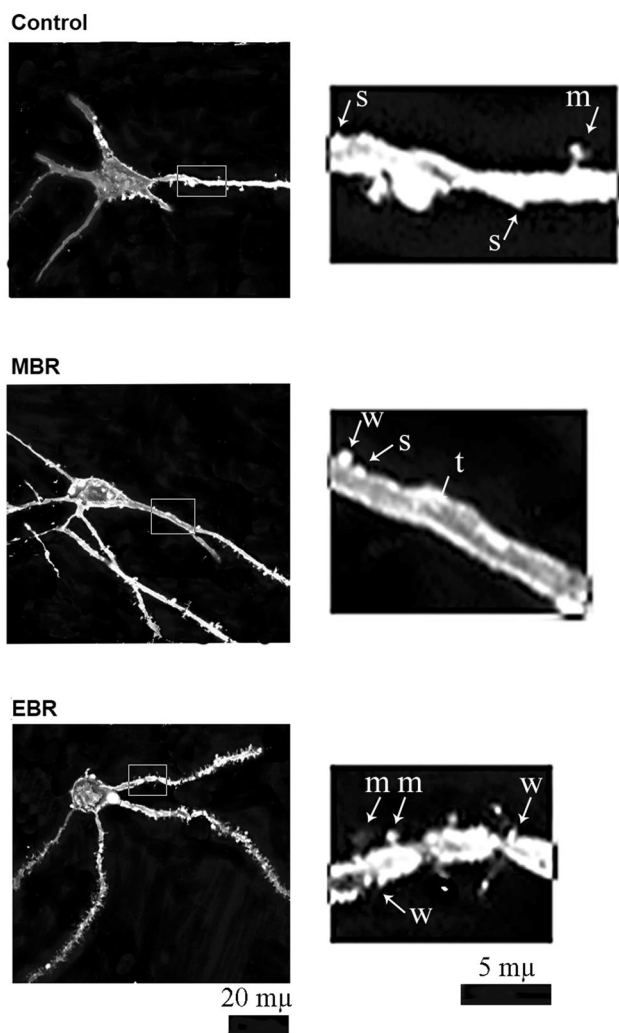


Fig. 6 Digitized fluorescent images of neurons labeled with Dil and reconstructed by confocal microscopy. Representative proximal dendritic branches showed pleomorphic spines in the basolateral amygdala of rats from control, MBR and EBR groups. Samples under higher magnification are shown on the right. *s* stubby, *t* thin, *m* mushroom, *w* wide

2014; van den Berk-Clark et al. 2018) and some suggest that overeating is an emotionally driven response (Carmassi et al. 2015).

In relation to the microPET-CT data some points should be mentioned: The normalization of 18 F-FDG data can be performed using different brain regions, however, some regions are classically used for normalization, such as the cerebellum or the whole brain (Platt et al. 2011; Poisnel et al. 2012; Li et al. 2016; Zanirati et al. 2018). In our study, no differences were found between the groups in either region. Thus, we chose to normalize the data based on the whole brain. Interestingly, a recent study showed that cerebellar structure and function are affected in PTSD patients (Holmes et al. 2018), which is in accordance with the idea

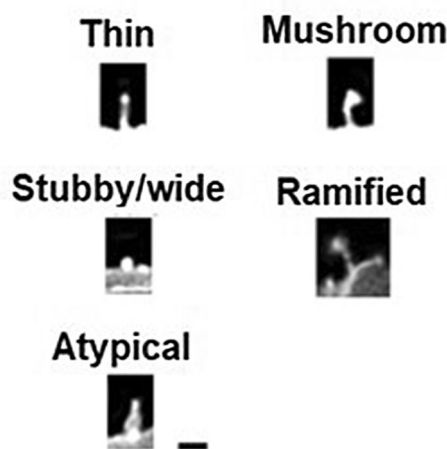


Fig. 7 Three-dimensional reconstructed images of dendritic spines from the BLA. Representative examples of each spine type according to their classification

that emotional context, such as stressful/aversive experiences, can affect the locomotor system (Metz et al. 2005). Transposing these findings to rodent models of PTSD, animals that received two intense electrical footshocks (1 mA, 60 Hz, 20 s) showed impaired walking adaptability (Medeiros et al. 2018). This evidence suggests that in a rodent model of PTSD, changes might be found in brain regions involved in posture and gait control, including the cerebellum. It should be noted that this model of PTSD is stronger than the model used in our study and no animals presented the MBR response (Medeiros et al. 2018). In our study, we adopted a weaker stress protocol to differentiate EBR and MBR responses, and no changes in cerebellar metabolism were found. While locomotion and gait were not assessed in our study, future studies comparing stronger versus weaker PTSD protocols and their effects on brain metabolism in regions involved in posture and gait control as well as on other locomotor parameters could be relevant to elucidate these points.

Our results show no alterations in the amygdala glucose metabolism between the experimental groups in either evaluation. Few studies have analyzed the encephalic metabolism in animal models of PTSD. A previous study by our research group shows a similar result 24 h after the situational reminder, thus, these findings corroborate the idea that PTSD does not produce a significant change in amygdala metabolism immediately or 24 h after the situational reminder (Saur et al. 2017). Additionally, our findings are in accordance with a recent study using microPET-FDG imaging which also reported unchanged amygdala glucose metabolism when comparing the animals' baseline scans with the scans realized immediately after the fear conditioning procedure and 1 week

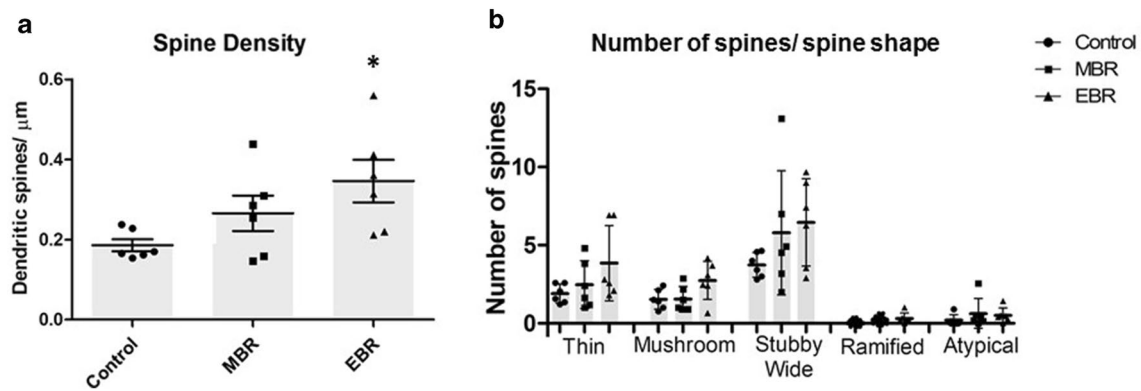


Fig. 8 Values (mean \pm SEM) for **a** the density of overall dendritic spines measured in the proximal 40 μ m and **b** the number of each dendritic spine type evaluated in the proximal 40 μ m in the basolateral amygdala neurons (BLA) * $p \leq 0.05$

later (Radford et al. 2018). On the other hand, a previous study, using a fear conditioning protocol which consisted of ten sets of tones (30 s, 75 dB) that co-terminated with a footshock (1 s, 0.5 mA) showed an increase in amygdala metabolism after this stress protocol (Zhu et al. 2016). It is possible that different stress intensities and frequencies, associated with an auditory stimulus might generate a more pronounced amygdala response and consequently an increase in amygdala glucose metabolism. Indeed, conditioning with different auditory stimuli may recruit distinct forms of synaptic plasticity and provide more malleable fear memory at least in the lateral amygdala of rats (Park et al. 2016). Changes in the amygdaloid glucose metabolism may be triggered by different kinds of perceived threat and maybe revealed using imaging techniques such as ^{18}F -FDG coupled to microPET-CT.

In clinical research, several conflicting results have been reported regarding the amygdala metabolism in patients with PTSD. Studies evaluating ^{18}F -FDG or cerebral blood flow (CBF) in this area show increased (Yehuda et al. 2009; Ramage et al. 2015; Vermetten et al. 2007), decreased (Yehuda et al. 2009; Buchsbaum et al. 2015; Stocker et al. 2014) and unaltered (Molina et al. 2010) glucose metabolism and CBF. These inconsistent findings may be due to the physiological complexity of PTSD and other factors should be considered such as the length of time since the onset of PTSD, different trauma type and severity and the distinct paradigms performed during the analyses (resting state, symptom provocation, trauma-related sensory stimuli).

Before discussing the dendritic spines, it is important to mention that, as previously cited in the “Materials and methods” section, some neurons could not be classified as either bitufted or stellate due to overlapping images. However, as they were almost certainly non-pyramidal neurons they were included in our analysis. Additionally, the clustering of these neurons is corroborated by the absence of any statistical difference in the density of dendritic spines, between

the types of neurons (bitufted, stellate and unclassified) (data not shown).

In our study, the number and shape of dendritic spines from BLA bitufted and stellate neurons were studied 1 day after exposure to the situational aversive reminder. We show in the EBR group, in which the animals exhibit more pronounced freezing behavior, there is an increased number of proximal dendritic spines. In all the studied groups, the freezing time is positively correlated with spine density. Our result is in accordance with a previous study where animals with extreme PTSD-like behavioral disruption demonstrated an increase in spine density and in dendritic arborization of BLA pyramidal neurons (Cohen et al. 2014). Furthermore, other studies evaluated the association between BLA neurons and emotional resilience and reported that individuals with more anxiety-like behaviors also showed higher BLA dendritic complexity and spine density (Mitra et al. 2009; Adamec et al. 2012; Hegde et al. 2017). The overall increase in the BLA spine density can be long-lasting (persisting for more than a month following the initial fear learning), susceptible to considerable plasticity and reversed by extinction training (Heinrichs et al. 2013). Other paradigms, such as chronic stress (Vyas et al. 2002, 2006; Mitra et al. 2005), early-life stress (Koe et al. 2016) or social stress (Patel et al. 2018), have been shown to induce increased spine density in BLA neurons associated with anxiety-like behaviors.

Together, these data show that in both BLA pyramidal and non-pyramidal neurons there are more dendritic spines in stressed animals, which suggests a higher synaptic input due to aversive stimulation. To modulate defensive behavior, the BLA neurons are connected to the hypothalamic regions (Petrovich et al. 2001). Thus, the experience-dependent plasticity of BLA neurons involves the perception of imminent threats and the adoption of defensive responses, such as freezing behavior (Janak and Tye 2015; Sah 2017). Hence, the BLA neurons would encode aversive learning in the fear/anxiety neural circuits

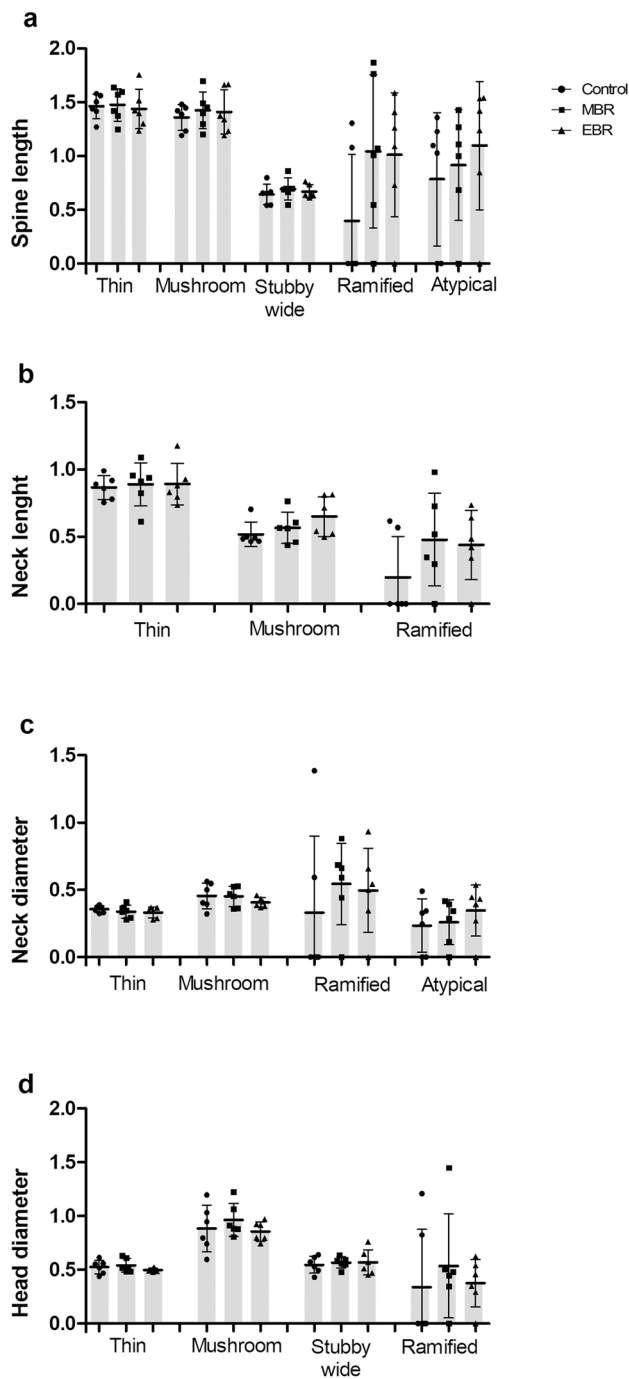


Fig. 9 Morphometric data (mean \pm SEM) regarding the **a** spine length; **b** neck length; **c** neck diameter and **d** head diameter measured in μm for the different spine types in the basolateral amygdala from each experimental group. Right-hand images exemplify each morphological parameter measured

by increasing the number of dendritic spines and the projections from these neurons reach downstream targets to modulate behavioral responses (Sah 2017). This would explain the strong response found in the EBR group when compared to the MBR group.

Notably, despite the overall increase in the number of dendritic spines, we found no specific class of dendritic spine was recruited more than any other. This suggests that irrespective of form and likely functions, spines of bitufted and stellate non-pyramidal neurons are similarly important for processing emotional information in the BLA. Likewise, the behavioral plasticity induced by our stress protocol is not associated with changes in a specific shape of dendritic spine or the structural morphometric parameter. This may be a task-specific feature which contrasts with the region-specific and spine-specific modulation of the synaptic plasticity that occurs in other amygdaloid areas, such as the posterodorsal medial amygdala (Zancan et al. 2018; Becker et al. 2017). Ultrastructural, optogenetic and electrophysiological approaches could be used to establish whether the proximal dendritic spines of different subpopulations of BLA neurons receive more excitatory or inhibitory contacts and the impact of this firing output in fear-conditioned rats.

Previous studies have provided reliable evidence regarding the effects of stress on spine morphology in different brain regions, such as the hippocampus and pre-frontal cortex (Sebastian et al. 2013; Radley et al. 2008).

In our study, we counted the number of different spine types in the BLA according to their morphology (thin, mushroom, stubby/wide, ramified and atypical) and measured their morphometrical data regarding spine length (SL); neck length (NL); head diameter (HD); and neck diameter (ND) in an animal model of PTSD.

Considering the dendritic spines, no statistical difference was found either in the number of each spine type or in any structural changes between the groups. Thus, we suppose that the behavioral plasticity induced by our stress protocol is not associated with morphological changes in spines or metabolic changes evaluated by microPET- ^{18}F -FDG.

Conclusions

In conclusion, our study demonstrates that animals exposed to the same situational trauma can express individual differences in their behavior, showing more or less susceptibility to the stress situation. Animals that showed extreme behavioral response (EBR) demonstrated an increase in proximal dendritic spine density in non-pyramidal BLA neurons with no alterations in the shape or morphometric parameters of the spines and no metabolic changes analyzed by microPET-FDG. We hope that our findings could help other researchers to understand the morphological bases of individual differences in the neurobiology underlying PTSD and other stress-related disorders.

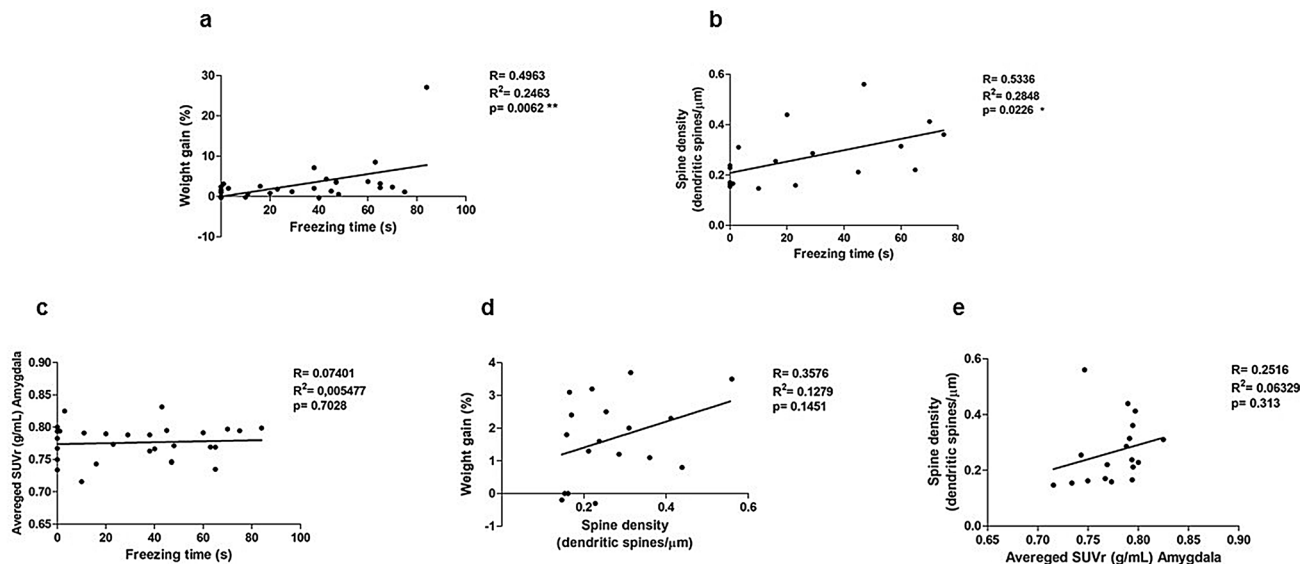


Fig. 10 This figure shows the results of the following Pearson's correlation tests: **a** freezing time and the percentage of body weight gain; **b** freezing time and spine density; **c** freezing time and ^{18}F -FDG activity; **d** spine density and the percentage of body weight gain

and **e** spine density and ^{18}F -FDG activity. Note a weak correlation ($R=0.4963$) between the freezing time and the percentage of body weight gain and a moderate correlation ($R=0.5336$) between freezing time and spine density

Acknowledgements This study was financed in part by the Coordenação de Aperfeiçoamento de Pessoal de Nível Superior—Brasil (CAPES)—Finance Code 001, Conselho Nacional de Pesquisa e Desenvolvimento (CNPq) and Fundação de Amparo à Pesquisa do Estado do Rio Grande do Sul (FAPERGS). JCC, AARF and LLX are CNPq investigators.

Author contributions LTN, LLX, AARF and RGM designed the study, interpreted the data and elaborated the manuscript. LTN, PFRN, LVP, BBM, GZL and RBS conducted the experimental procedures. LTN, MZ, MMBPO, LVP and PFRN collected and interpreted the data. LTN, GTV, SG and JCC conducted the microPET-FDG scans and analysis.

Funding This study was financed by the Coordenação de Aperfeiçoamento de Pessoal de Nível Superior—Brasil (CAPES) (Finance Code 001), Conselho Nacional de Pesquisa e Desenvolvimento (CNPq) (Grant Number 306644/2016-9) and Fundação de Amparo à Pesquisa do Estado do Rio Grande do Sul (FAPERGS) (Grant Number 04/1037.1).

Compliance with ethical standards

Conflict of interest The authors declare that there are no conflicts of interest.

Ethical approval All applicable international, national, and institutional guidelines for the care and use of animals were followed. All experiments involving animals were approved by the University's ethical committee (CEUA 8481/PUCRS).

References

- Adamec R, Hebert M, Blundell J, Mervis RF (2012) Dendritic morphology of amygdala and hippocampal neurons in more and less predator stress responsive rats and more and less spontaneously anxious handled controls. *Behav Brain Res*. <https://doi.org/10.1016/j.bbr.2011.09.009>
- American Psychiatric Association (2013) Diagnostic and statistical manual of mental disorders: DSM-5, 5th edn. American Psychiatric Association, Washington
- Arellano JI, Espinosa A, Fairén A, Yuste R, DeFelipe J (2007) Non-synaptic dendritic spines in neocortex. *Neuroscience* 145:464–469. <https://doi.org/10.1016/j.neuroscience.2006.12.015>
- Baptista PPA, Saur L, Bagatini PB, Greggio S, Venturin GT, Vaz SP, dos R. Ferreira K, Junqueira JS, Lara DR, DaCosta JC, Jeckel CMM, Mestriner RG, Xavier LL (2015) Antidepressant effects of ketamine are not related to ^{18}F -FDG metabolism or tyrosine hydroxylase immunoreactivity in the ventral tegmental area of Wistar rats. *Neurochem Res* 40:1153–1164. <https://doi.org/10.1007/s11064-015-1576-3>
- Becker RO, Rasia-Filho AA, Giovenardi M (2017) Selective deletion of the oxytocin gene remodels the number and shape of dendritic spines in the medial amygdala of males with and without sexual experience. *Neurosci Lett* 660:155–159. <https://doi.org/10.1016/j.neulet.2017.08.075>
- Benjet C, Bromet E, Karam EG, Kessler RC, McLaughlin KA, Rusico AM, Shahly V, Stein DJ, Petukhova M, Hill E, Alonso J, Atwoli L, Bunting B, De Girolamo G, Florescu S, Gureje O, Lepine JP, Kawakami N, Kovess-masfety V, Medina-Mora M, Navarro-Mateu F, Piazza M, Posada-Villa J, Scott K, Shalev A, Slade T, ten Have M, Torres Y, Viana M, Zarkov Z, Koenen K (2016) The epidemiology of traumatic event exposure worldwide: results. *Psychol Med* 46:327–343. <https://doi.org/10.1017/S0033291715001981.The>
- Borghans B (2015) Animal models for posttraumatic stress disorder: an overview of what is used in research. *World J Psychiatry* 5:387. <https://doi.org/10.5498/wjp.v5.i4.387>

- Bourne J, Harris KM (2007) Do thin spines learn to be mushroom spines that remember? *Curr Opin Neurobiol* 17:381–386. <https://doi.org/10.1016/j.conb.2007.04.009>
- Brusco J, Dall'Oglio A, Rocha LB, Rossi MA, Moreira JE, Rasia-Filho AA (2010) Descriptive findings on the morphology of dendritic spines in the rat medial amygdala. *Neurosci Lett* 483:152–156. <https://doi.org/10.1016/j.neulet.2010.07.083>
- Brusco J, Merlo S, Ikeda ET, Petralia RS, Kachar B, Rasia-Filho AA, Moreira JE (2014) Inhibitory and multisynaptic spines, and hemispherical synaptic specialization in the posterodorsal medial amygdala of male and female rats. *J Comp Neurol* 522:2075–2088. <https://doi.org/10.1002/cne.23518>
- Buchsbaum MS, Simmons AN, DeCastro A, Farid N, Matthews SC (2015) Clusters of low ¹⁸F-fluorodeoxyglucose uptake voxels in combat veterans with traumatic brain injury and post-traumatic stress disorder. *J Neurotrauma* 32:1736–1750. <https://doi.org/10.1099/vir.0.81055-0>
- Bush DEA, Sotres-Bayon F, LeDoux JE (2007) Individual differences in fear: isolating fear reactivity and fear recovery phenotypes. *J Trauma Stress* 20:413–422. <https://doi.org/10.1002/jts.20261>
- Carmassi C, Antonio Bertelloni C, Massimetti G, Miniati M, Stratta P, Rossi A, Dell'Osso L (2015) Impact of DSM-5 PTSD and gender on impaired eating behaviors in 512 Italian earthquake survivors. *Psychiatry Res* 225:64–69. <https://doi.org/10.1016/j.psychres.2014.10.008>
- Chen Y, Sabatini BL (2012) Signaling in dendritic spines and spine microdomains. *Curr Opin Neurobiol* 22:389–396. <https://doi.org/10.1016/j.conb.2012.03.003>
- Cohen H, Zohar J, Matar M (2003) The relevance of differential response to trauma in an animal model of posttraumatic stress disorder. *Biol Psychiatry* 53:463–473. [https://doi.org/10.1016/S0006-3223\(02\)01909-1](https://doi.org/10.1016/S0006-3223(02)01909-1)
- Cohen H, Zohar J, Matar MA, Zeev K, Loewenthal U, Richter-Levin G (2004) Setting apart the affected: the use of behavioral criteria in animal models of post traumatic stress disorder. *Neuropsychopharmacology* 29:1962. <https://doi.org/10.1038/sj.npp.1300523>
- Cohen H, Kozlovsky N, Matar MA, Zohar J, Kaplan Z (2014) Distinctive hippocampal and amygdalar cytoarchitectural changes underlie specific patterns of behavioral disruption following stress exposure in an animal model of PTSD. *Eur Neuropsychopharmacol*. <https://doi.org/10.1016/j.euroneuro.2014.09.009>
- Cooke BM, Woolley CS (2005) Sexually dimorphic synaptic organization of the medial amygdala. *J Neurosci* 25:10759–10767. <https://doi.org/10.1523/jneurosci.2919-05.2005>
- Dall'Oglio A, Dutra ACL, Moreira JE, Rasia-Filho AA (2015) The human medial amygdala: Structure, diversity, and complexity of dendritic spines. *J Anat* 227:440–459. <https://doi.org/10.1111/joa.12358>
- Dalpian F, Brusco J, Calcagnotto ME, Moreira JE, Rasia-Filho AA (2015) Distribution of glutamate receptors in the posterodorsal medial amygdala of adult male rats. *Histol Histopathol* 30:1303–1311. <https://doi.org/10.14670/HH-11-626>
- de Castilhos J, Forti CD, Achaval M, Rasia-Filho AA (2008) Dendritic spine density of posterodorsal medial amygdala neurons can be affected by gonadectomy and sex steroid manipulations in adult rats: a Golgi study. *Brain Res* 1240:73–81. <https://doi.org/10.1016/j.brainres.2008.09.002>
- Diehl LA, Silveira PP, Leite MC, Crema LM, Portella AK, Billodre MN, Nunes E, Henriques TP, Fidelix-da-Silva LB, Heis MD, Gonçalves CA, Quillfeldt JA, Dalmaz C (2007) Long lasting sex-specific effects upon behavior and S100b levels after maternal separation and exposure to a model of post-traumatic stress disorder in rats. *Brain Res* 1144:107–116. <https://doi.org/10.1016/j.brainres.2007.01.084>
- Fanselow MS (1994) Neural organization of the defensive behavior system responsible for fear. *Psychon Bull Rev* 1:429–438. <https://doi.org/10.3758/BF03210947>
- Fenster RJ, Lebois LAM, Ressler KJ, Suh J (2018) Brain circuit dysfunction in post-traumatic stress disorder: from mouse to man. *Nat Rev Neurosci* 9:535–551. <https://doi.org/10.1016/j.celrep.2015.11.047.Long>
- Flandreau EI, Toth M (2017) Animal models of PTSD: a critical review. *Curr Top Behav Neurosci* 38:47–68. https://doi.org/10.1007/7854_2016_65
- Gipson CD, Olive MF (2017) Structural and functional plasticity of dendritic spines—root or result of behavior? *Genes Brain Behav* 16:101–117. <https://doi.org/10.1111/gbb.12324>
- Goto T, Kubota Y, Tanaka Y, Iio W, Moriya N, Toyoda A (2014) Subchronic and mild social defeat stress accelerates food intake and body weight gain with polydipsia-like features in mice. *Behav Brain Res* 270:339–348. <https://doi.org/10.1016/j.bbr.2014.05.040>
- Harris KM, Jensen FE, Tsao B (1992) Three-dimensional structure of dendritic spines and synapses in rat hippocampus (CA1) at postnatal day 15 and adult ages: implications for the maturation of synaptic physiology and long-term potentiation. *J Neurosci* 12:2685–2705
- Heck N, Betuing S, Vanhoutte P, Caboche J (2012) A deconvolution method to improve automated 3D-analysis of dendritic spines: application to a mouse model of Huntington's disease. *Brain Struct Funct* 217:421–434. <https://doi.org/10.1007/s00429-011-0340-y>
- Hegde A, Soh Yee P, Mitra R (2017) Dendritic architecture of principal basolateral amygdala neurons changes congruently with endocrine response to stress. *Int J Environ Res Public Health* 14:779. <https://doi.org/10.3390/ijerph14070779>
- Heim C, Nemeroff CB (2001) The role of childhood trauma in the neurobiology of mood and anxiety disorders: preclinical and clinical studies. *Biol Psychiatry* 49:1023–1039
- Heinrichs SC, Leite-Morris KA, Guy MD, Goldberg LR, Young AJ, Kaplan GB (2013) Dendritic structural plasticity in the basolateral amygdala after fear conditioning and its extinction in mice. *Behav Brain Res*. <https://doi.org/10.1016/j.bbr.2013.03.048>
- Holmes SE, Scheinost D, DellaGioia N, Davis MT, Matuskey D, Pietrzak RH, Hampson M, Krystal JH, Esterlis I (2018) Cerebellar and prefrontal cortical alterations in PTSD: structural and functional evidence. *Chronic Stress (Thousand Oaks)*. <https://doi.org/10.1177/2470547018786390>
- Janak PH, Tye KM (2015) From circuits to behaviour in the amygdala. *Nature* 517:284–292. <https://doi.org/10.1038/nature14188>
- Jiang X, Zhang ZJ, Zhang S, Gamble EH, Min Jia RJ, Ursano H Li (2011) 5-HT 2A receptor antagonism by MDL 11,939 during inescapable stress prevents subsequent exaggeration of acoustic startle response and reduced body weight in rats. *J Psychopharmacol* 25:287–295. <https://doi.org/10.1177/0269881109106911>
- Kessler RC, Sonnega A, Bromet E, Hughes KC, Nelson B (1995) Posttraumatic stress disorder in the National Comorbidity Survey. *Arch Gen Psychiatry* 52:1048–1060. <https://doi.org/10.1001/archpsyc.1995.03950240066012>
- Koe AS, Ashokan A, Mitra R (2016) Short environmental enrichment in adulthood reverses anxiety and basolateral amygdala hypertrophy induced by maternal separation. *Transl Psychiatry* 6:e729. <https://doi.org/10.1038/tp.2015.217>
- Krishnan V, Han M-H, Graham DL, Berton O, Renthal W, Russo SJ, LaPlant Q, Graham A, Lutter M, Lagace DC, Ghose S, Reister R, Tannous P, Green TA, Neve RL, Chakravarty S, Kumar A, Eisch AJ, Self DW, Lee FS, Tamminga CA, Cooper DC, Gershenfeld HK, Nestler EJ (2007) Molecular adaptations underlying susceptibility and resistance to social defeat in brain reward regions. *Cell* 131:391–404. <https://doi.org/10.1016/j.cell.2007.09.018>

- Kubzansky LD, Bordelois P, Jun HJ, Roberts AL, Cerda M, Bluestone N, Koenen KC (2014) The weight of traumatic stress: a prospective study of posttraumatic stress disorder symptoms and weight status in women. *JAMA Psychiatry* 71:44–51. <https://doi.org/10.1001/jamapsychiatry.2013.2798>
- Lancelot S, Zimmer L (2010) Small-animal positron emission tomography as a tool for neuropharmacology. *Trends Pharmacol Sci* 31:411–417. <https://doi.org/10.1016/j.tips.2010.06.002>
- Leuner B, Shors TJ (2013) Stress, anxiety, and dendritic spines: what are the connections? *Neuroscience*. <https://doi.org/10.1016/j.neuroscience.2012.04.021>
- Li XY, Men WW, Zhu H, Lei JF, Zuo FX, Wang ZJ, Zhu ZH, Bao XJ, Wang RZ (2016) Age- and brain region-specific changes of glucose metabolic disorder, learning, and memory dysfunction in early Alzheimer's disease assessed in APP/PS1 transgenic mice using ¹⁸F-FDG-PET. *Int J Mol Sci*. <https://doi.org/10.3390/ijms17101707>
- Luczynski P, Whelan SO, O'Sullivan C, Clarke G, Shanahan F, Dinan TG, Cryan JF (2016) Adult microbiota-deficient mice have distinct dendritic morphological changes: differential effects in the amygdala and hippocampus. *Eur J Neurosci* 44:2654–2666. <https://doi.org/10.1111/ejn.13291>
- Malan-Muller S, Valles-Colomer M, Raes J, Lowry CA, Seedat S, Hemmings SMJ (2018) The gut microbiome and mental health: implications for anxiety- and trauma-related disorders. *Omi A J Integr Biol* 22:90–107. <https://doi.org/10.1089/omi.2017.0077>
- McEwen BS (2008) Central effects of stress hormones in health and disease: understanding the protective and damaging effects of stress and stress mediators. *Eur J Pharmacol* 583:174–185. <https://doi.org/10.1016/j.ejphar.2007.11.071>
- Medeiros FM, de Carvalho Myskiw J, Baptista PPA, Neves LT, Martins LA, Furini CRG, Izquierdo I, Xavier LL, Hollands K, Mestriner RG (2018) Can an aversive, extinction-resistant memory trigger impairments in walking adaptability? An experimental study using adult rats. *Neurosci Lett* 665:224–228. <https://doi.org/10.1016/j.neulet.2017.12.017>
- Metz GA, Jadavji NM, Smith LK (2005) Modulation of motor function by stress: a novel concept of the effects of stress and corticosterone on behavior. *Eur J Neurosci* 22:1190–1200. <https://doi.org/10.1111/j.1460-9568.2005.04285.x>
- Mitra R, Sapolsky RM (2008) Acute corticosterone treatment is sufficient to induce anxiety and amygdaloid dendritic hypertrophy. *Proc Natl Acad Sci USA* 105:5573–5578. <https://doi.org/10.1073/pnas.0705615105>
- Mitra R, Jadhav S, McEwen BS, Vyas A, Chattarji S (2005) Stress duration modulates the spatiotemporal patterns of spine formation in the basolateral amygdala. *Proc Natl Acad Sci*. <https://doi.org/10.1073/pnas.0504011102>
- Mitra R, Ferguson D, Sapolsky RM (2009) SK2 potassium channel overexpression in basolateral amygdala reduces anxiety, stress-induced corticosterone secretion and dendritic arborization. *Mol Psychiatry* 14:827, 847–855. <https://doi.org/10.1038/mp.2009.9>
- Molina ME, Isoardi R, Prado MN, Bentolila S (2010) Basal cerebral glucose distribution in long-term post-traumatic stress disorder. *World J Biol Psychiatry* 11:493–501. <https://doi.org/10.3109/15622970701472094>
- Mongeau R, Miller GA, Chiang E, Anderson DJ (2003) Neural correlates of competing fear behaviors evoked by an innately aversive stimulus. *J Neurosci* 23:3855–3868. <https://doi.org/10.1523/JNEUROSCI.23-09-03855.2003>
- Musazzi L, Tornese P, Sala N, Popoli M (2018) What acute stress protocols can tell us about PTSD and stress-related neuropsychiatric disorders. *Front Pharmacol* 9:1–13. <https://doi.org/10.3389/fphar.2018.00758>
- Park S, Lee J, Park K, Kim J, Song B, Hong I, Kim J, Lee S, Choi S (2016) Sound tuning of amygdala plasticity in auditory fear conditioning. *Sci Rep* 6:1–14. <https://doi.org/10.1038/srep31069>
- Patel D, Anilkumar S, Chattarji S, Buwalda B (2018) Repeated social stress leads to contrasting patterns of structural plasticity in the amygdala and hippocampus. *Behav Brain Res* 347:314–324. <https://doi.org/10.1016/j.bbr.2018.03.034>
- Paxinos G, Watson C (2014) *The rat brain in stereotaxic coordinates*. 7th edn. Elsevier, London
- Petrovich GD, Canteras NS, Swanson LW (2001) Combinatorial amygdalar inputs to hippocampal domains and hypothalamic behavior systems. *Brain Res Rev* 38:247–289
- Platt B, Drever B, Koss D, Stoppelkamp S, Jyoti A, Plano A, Utan A, Merrick G, Ryan D, Melis V, Wan H, Mingarelli M, Porcu E, Scrocchi L, Welch A, Riedel G (2011) Abnormal cognition, sleep, eeg and brain metabolism in a novel knock-in Alzheimer mouse, plb1. *PLoS One*. <https://doi.org/10.1371/journal.pone.0027068>
- Poisnel G, Hérard AS, El Tannir El N, Tayara E, Bourrin A, Volk F, Kober B, Delatour T, Delzescaux T, Debeir T, Rooney J, Benavides P, Hantraye M Dhenain (2012) Increased regional cerebral glucose uptake in an APP/PS1 model of Alzheimer's disease. *Neurobiol Aging* 33:1995–2005. <https://doi.org/10.1016/j.neurobiolaging.2011.09.026>
- Radford KD, Park TY, Jaiswal S, Pan H, Knutsen A, Zhang M, Driscoll M, Osborne-Smith LA, Dardzinski BJ, Choi KH (2018) Enhanced fear memories and brain glucose metabolism (¹⁸F-FDG-PET) following sub-anesthetic intravenous ketamine infusion in Sprague-Dawley rats. *Transl Psychiatry* 8:263. <https://doi.org/10.1038/s41398-018-0310-8>
- Radley JJ, Rocher AB, Rodriguez A, Ehlenberger DB, Dammann M, McEwen BS, Morrison JH, Wearne SL, Hof PR (2008) Repeated stress alters dendritic spine morphology in the rat medial prefrontal cortex. *J Comp Neurol* 507:1141–1150. <https://doi.org/10.1002/cne.21588>
- Ramage AE, Litz BT, Resick PA, Woolsey MD, Dondanville KA, Young-McCaughan S, Borah AM, Borah EV, Peterson AL, Fox PT (2015) Regional cerebral glucose metabolism differentiates danger- and non-danger-based traumas in post-traumatic stress disorder. *Soc Cogn Affect Neurosci* 11:234–242. <https://doi.org/10.1093/scan/nsv102>
- Rasia-Filho AR-F (2010) Dendritic spines observed by extracellular Dil dye and immunolabeling under confocal microscopy. *Protoc Exch*. <https://doi.org/10.1038/nprot.2010.153>
- Rasia-Filho AA, Londero RG, Achaval M (2000) Functional activities of the amygdala: an overview Canadian Medical Association. *J Psychiatry Neurosci* 25:14–23. <https://www.ncbi.nlm.nih.gov/pmc/articles/PMC1407702/pdf/jpn00084-0020.pdf>
- Rasia-Filho AA, Fabian C, Rigoti KM, Achaval M (2004) Influence of sex, estrous cycle and motherhood on dendritic spine density in the rat medial amygdala revealed by the Golgi method. *Neuroscience* 126:839–847. <https://doi.org/10.1016/j.neuroscience.2004.04.009>
- Rauch SL, Whalen PJ, Shin LM, McInerney SC, Macklin ML, Lasko NB, Orr SP, Pitman RK (2000) Exaggerated amygdala response to masked facial stimuli in posttraumatic stress disorder: a functional MRI study. *Biol Psychiatry* 47:769–776
- Ryu J, Liu L, Wong TP, Wu DC, Burette A, Weinberg R, Wang YT, Sheng M (2006) A critical role for myosin IIB in dendritic spine morphology and synaptic function. *Neuron* 49:175–182. <https://doi.org/10.1016/j.neuron.2005.12.017>
- Sah P (2017) Fear, anxiety, and the amygdala. *Neuron* 96:1–2. <https://doi.org/10.1016/j.neuron.2017.09.013>
- Saur L, Baptista PPA, Bagatini PB, Neves LT, de Oliveira RM, Vaz SP, Ferreira K, Machado SA, Mestriner RG, Xavier LL (2016) Experimental post-traumatic stress disorder decreases astrocyte

- density and changes astrocytic polarity in the CA1 hippocampus of male rats. *Neurochem Res* 41:892–904. <https://doi.org/10.1007/s11064-015-1770-3>
- Saur L, Neves LT, Greggio S, Venturin GT, Jeckel CMM, Costa Da Costa J, Bertoldi K, Schallenger B, Siqueira IR, Mestriner RG, Xavier LL (2017) Ketamine promotes increased freezing behavior in rats with experimental PTSD without changing brain glucose metabolism or BDNF. *Neurosci Lett* 658:6–11. <https://doi.org/10.1016/j.neulet.2017.08.026>
- Sebastian V, Estil JB, Chen D, Schrott LM, Serrano PA (2013) Acute physiological stress promotes clustering of synaptic markers and alters spine morphology in the hippocampus. *PLoS One* 8:1–14. <https://doi.org/10.1371/journal.pone.0079077>
- Shalev A, Liberzon I, Marmar C (2017) Posttraumatic stress disorder. *N Engl J Med* 376:2459–2469. <https://doi.org/10.1016/B978-0-12-803457-6.00013-1>
- Shin LM, Wright CI, Cannistraro PA, Wedig MM, McMullin K, Martis B, Macklin ML, Lasko NB, Cavanagh SR, Krangel TS, Orr SP, Pitman RK, Whalen PJ, Rauch SL (2005) A functional magnetic resonance imaging study of amygdala and medial prefrontal cortex responses to overtly presented fearful faces in posttraumatic stress disorder. *Arch Gen Psychiatry* 62:273–281. <https://doi.org/10.1001/archpsyc.62.3.273>
- Shu Y, Xu T (2017) Chronic social defeat stress modulates dendritic spines structural plasticity in adult mouse frontal association cortex. *Neural Plast*. <https://doi.org/10.1155/2017/6207873>
- Silva BA, Gross CT, Gräff J (2016) The neural circuits of innate fear: detection, integration, action, and memorization. *Learn Mem* 23:544–555. <https://doi.org/10.1101/lm.042812.116>
- Stewart MG, Popov VI, Kraev IV, Medvedev N, Davies HA (2014) Structure and complexity of the synapse and dendritic spine. *The synapse*. Academic Press, New York, pp 1–20
- Stocker RPI, Cieply MA, Paul B, Khan H, Henry L, Kontos AP, Germain A (2014) Combat-related blast exposure and traumatic brain injury influence brain glucose metabolism during REM sleep in military veterans. *Neuroimage* 99:207–214. <https://doi.org/10.1016/j.neuroimage.2014.05.067>
- Tovote P, Fadok JP, Lüthi A (2015) Neuronal circuits for fear and anxiety. *Nat Rev Neurosci* 16:317–331. <https://doi.org/10.1038/nrn3945>
- Vallès A, Martí O, García A, Armario A (2000) Single exposure to stressors causes long-lasting, stress-dependent reduction of food intake in rats. *Am J Physiol Regul Integr Comp Physiol* 279:R1138–R1144. <https://doi.org/10.1152/ajpregu.2000.279.3.R1138>
- van den Berk-Clark C, Secrest S, Walls J, Hallberg E, Lustman PJ, Schneider FD, Scherrer JF (2018) Association between posttraumatic stress disorder and lack of exercise, poor diet, obesity, and co-occurring smoking: a systematic review and meta-analysis. *Health Psychol* 37:407–416. <https://doi.org/10.1037/hea0000593>
- Vermetten E, Schmahl C, Southwick SM, Bremner JD (2007) Positron tomographic emission study of olfactory induced emotional recall in veterans with and without combat-related posttraumatic stress disorder. *Psychopharmacol Bull* 40:8–30. <https://www.ncbi.nlm.nih.gov/pubmed/17285093>
- Virdee K, Cumming P, Caprioli D, Jupp B, Rominger A, Aigbirhio FI, Fryer TD, Riss PJ, Dalley JW (2012) Applications of positron emission tomography in animal models of neurological and neuropsychiatric disorders. *Neurosci Biobehav Rev* 36:1188–1216. <https://doi.org/10.1016/j.neubiorev.2012.01.009>
- Vyas A, Mitra R, Shankaranarayana Rao BS, Chattarji S (2002) Chronic stress induces contrasting patterns of dendritic remodeling in hippocampal and amygdaloid neurons. *J Neurosci* 22:6810–6818
- Vyas A, Pillai AG, Chattarji S (2004) Recovery after chronic stress fails to reverse amygdaloid neuronal hypertrophy and enhanced anxiety-like behavior. *Neuroscience*. <https://doi.org/10.1016/j.neuroscience.2004.07.013>
- Vyas A, Jadhav S, Chattarji S (2006) Prolonged behavioral stress enhances synaptic connectivity in the basolateral amygdala. *Neuroscience*. <https://doi.org/10.1016/j.neuroscience.2006.08.003>
- Wei P, Liu N, Zhang Z, Liu X, Tang Y, He X, Wu B, Zhou Z, Liu Y, Li J, Zhang Y, Zhou X, Xu L, Chen L, Bi G, Hu X, Xu F, Wang L (2015) Processing of visually evoked innate fear by a non-canonical thalamic pathway. *Nat Commun* 6:1–12. <https://doi.org/10.1038/ncomms7756>
- Yehuda R, Harvey PD, Golier JA, Newmark RE, Bowie CR, Wohltmann JJ, Grossman RA, Schmeidler J, Hazlett EA, Buchsbaum MS (2009) Changes in relative glucose metabolic rate following cortisol administration in aging veterans with posttraumatic stress disorder: an FDG-PET neuroimaging study. *J Neuropsychiatry Clin Neurosci*. <https://doi.org/10.1176/jnp.2009.21.2.132>
- Yehuda R, Hoge CW, McFarlane AC, Vermetten E, Lanius RA, Niv-ergelt CM, Hobfoll SE, Koenen KC, Neylan TC, Hyman SE (2015) Post-traumatic stress disorder. *Nat Rev Dis Prim* 1:15057. <https://doi.org/10.1038/nrdp.2015.57>
- Yuste R (2013) Electrical compartmentalization in dendritic spines. *Annu Rev Neurosci* 36:429–449. <https://doi.org/10.1146/annurev-neuro-062111-150455>
- Zancan M, Dall'Oglio A, Quagliotto E, Rasia-Filho AA (2017) Castration alters the number and structure of dendritic spines in the male posterodorsal medial amygdala. *Eur J Neurosci* 45:572–580. <https://doi.org/10.1111/ejn.13460>
- Zancan M, da Cunha RSR, Schroeder F, Xavier LL, Rasia-Filho AA (2018) Remodeling of the number and structure of dendritic spines in the medial amygdala: from prepubertal sexual dimorphism to puberty and effect of sexual experience in male rats. *Eur J Neurosci* 48:1851–1865. <https://doi.org/10.1111/ejn.14052>
- Zanirati G, Azevedo PN, Venturin GT, Greggio S, Alcará AM, Zimmer ER, Feltes PK, DaCosta JC (2018) Depression comorbidity in epileptic rats is related to brain glucose hypometabolism and hypersynchronicity in the metabolic network architecture. *Epilepsia* 59:923–934. <https://doi.org/10.1111/epi.14057>
- Zhang JY, Liu TH, He Y, Pan HQ, Zhang WH, Yin XP, Tian XL, Li BM, Wang XD, Holmes A, Yuan TF, Pan BX (2018) Chronic stress remodels synapses in an amygdala circuit-specific manner. *Biol Psychiatry*. <https://doi.org/10.1016/j.biopsych.2018.06.019>
- Zhu Y, Du R, Zhu Y, Shen Y, Zhang K, Chen Y, Song F, Wu S, Zhang H, Tian M (2016) PET mapping of neurofunctional changes in a posttraumatic stress disorder model. *J Nucl Med* 57:1474–1477. <https://doi.org/10.2967/jnumed.116.173443>

Publisher's Note Springer Nature remains neutral with regard to jurisdictional claims in published maps and institutional affiliations.